International Journal of Chemical, Materials and Biomolecular Sciences
ISSN: 2415-6620
Vol:14, No:9, 2020

Effects of Level Densities and Those of a-Parameter in the Framework of Preequilibrium Model for ^{63,65}Cu(n,xp) Reactions in Neutrons at 9 to 15 MeV

L. Yettou

***Abstract*—**In this study, the calculations of proton emission spectra produced by ^{63}Cu(n,xp) and ^{65}Cu(n,xp) reactions are used in the framework of preequilibrium models using the EMPIRE code and TALYS code. Exciton Model predidtions combined with the Kalbach angular distribution systematics and the Hybrid Monte Carlo Simulation (HMS) were used. The effects of levels densities and those of a-parameter have been investigated for our calculations. The comparison with experimental data shows clear improvement over the Exciton Model and HMS calculations.

***Keywords*—**Preequilibrium models, level density, level density a-parameter, ^{63}Cu(n,xp) and ^{65}Cu(n,xp) reactions.

I. Introduction

THE calculations of proton emission spectra produced by (n, xp) reactions are indispensable for design of nuclear devices and the development of high quality nuclear data of copper is particularly important due to its role as an important structural material in many accelerator-driven system designs. Natural copper consists of two isotopes, that is ^{63}Cu (69, 17%) and ^{65}Cu (30, 83%). In this work, a consistent selection of preequilibrium models, statistical model, optical model and level densities represent the physics core in present calculation. The cross sections for the emission of proton on ^{63}Cu and ^{65}Cu are calculated for incident neutron energies of 9, 11, 14.8, and 15 MeV in the framework of preequilibrium and equilibrium models using EMPIRE 3.2 code [1] and TALYS 1.8 code [2], where the sensitivity of some parameters as the level density, level density a-parameter and optical model are considered. Some input parameters as spin cutoff parameter, single-particle level density *g*, mean free path, pairing correction, M2constant, M2limit and M2shift from squared matrix element have been taken in account in our calculations using EMPIRE 3.2 code [1] and TALYS 1.8 code [2], but not shown in this work. The detailed description is given in [3], [4].

II. Formula of Theoretical Models

The phenomenological pre-equilibrium mechanism as defined by [5] is the exciton model. Two versions of the exciton model are implemented in TALYS code [2]: the default is the two-component model in which the neutron or proton particles and holes are followed throughout the reaction. The preequilibrium differential cross section for the emission of a particle k with emission energy E_k can be expressed in terms of the lifetime of exciton state (p_π, h_π, p_ν, h_ν) τ, the composite nucleus formation cross section σ_{CF}, and an emission rate W_k

$$\frac{d\sigma_k^{PE}}{dE_k} = \sigma^{CF} \sum_{p_\pi=p_\pi^0}^{p_\pi^{max}} \sum_{p_\nu=p_\nu^0}^{p_\nu^{max}} W_k(p_\pi, h_\pi, p_\nu, h_\nu, E_k)\, \tau(p_\pi, h_\pi, p_\nu, h_\nu) \times P(p_\pi, h_\pi, p_\nu, h_\nu) \quad (1)$$

where the factor P represents the part of the preequilibrium population that has survived emission from the previous states and passes through the (p_π, h_π, p_ν, h_ν) configurations, averaged over time. The lifetime τ of exciton state (p_π, h_π, p_ν, h_ν) in (1) is defined as the inverse sum of the total emission rate and the various internal transition rates

$$\tau(p_\pi, h_\pi, p_\nu, h_\nu) = \begin{bmatrix} \lambda_\pi^+(p_\pi, h_\pi, p_\nu, h_\nu) + \lambda_\nu^+(p_\pi, h_\pi, p_\nu, h_\nu) + \\ \lambda_{\pi\nu}^0(p_\pi, h_\pi, p_\nu, h_\nu) + \lambda_{\nu\pi}^0(p_\pi, h_\pi, p_\nu, h_\nu) + \\ W(p_\pi, h_\pi, p_\nu, h_\nu) \end{bmatrix}^{-1} \quad (2)$$

In the one-component exciton model as implemented in PCROSS module of EMPIRE [1], the phenomenological pre-equilibrium mechanism as defined by [5] is based on the solution of the master equation [6] proposed by [7] and [8]. The pre-equilibrium spectra in this model are given as:

$$\frac{d\sigma_{a,b}}{d\epsilon_b}(\epsilon_b) = \sigma_{a,b}^r(E_{inc}) D_{a,b}(E_{inc}) \times \sum_n W_b(E, n, \epsilon_b)\tau(n) \quad (3)$$

where ϵ_b is the emission energy for the emission of a particle b, $\sigma_{a,b}^r(E_{inc})$ the cross section of the reaction (a, b), $W_b(E, n, \epsilon_b)$ the probability of emission of a particle of type b (or gamma ray) with energy ϵ_b from a state with n excitons and excitation energy E of the compound nucleus, and $D_{a,b}(E_{inc})$ the depletion factor which takes into account the decrease in the available cross section due to the particle emission by direct interaction with low excitation energy levels of the target nucleus and given by

$$D_{a,b}(E_{inc}) = 1 - \frac{\sigma_{a,b}^{dir}(E_{inc})}{\sigma_{a,b}^r(E_{inc})} \quad (4)$$

where $\sigma_{a,b}^{dir}(E_{inc})$ is the direct reaction cross section.

Leila Yettou is with the University of Bab Ezzouar USTHB, Algeria (e-mail: leilayettou448@hotmail.com).

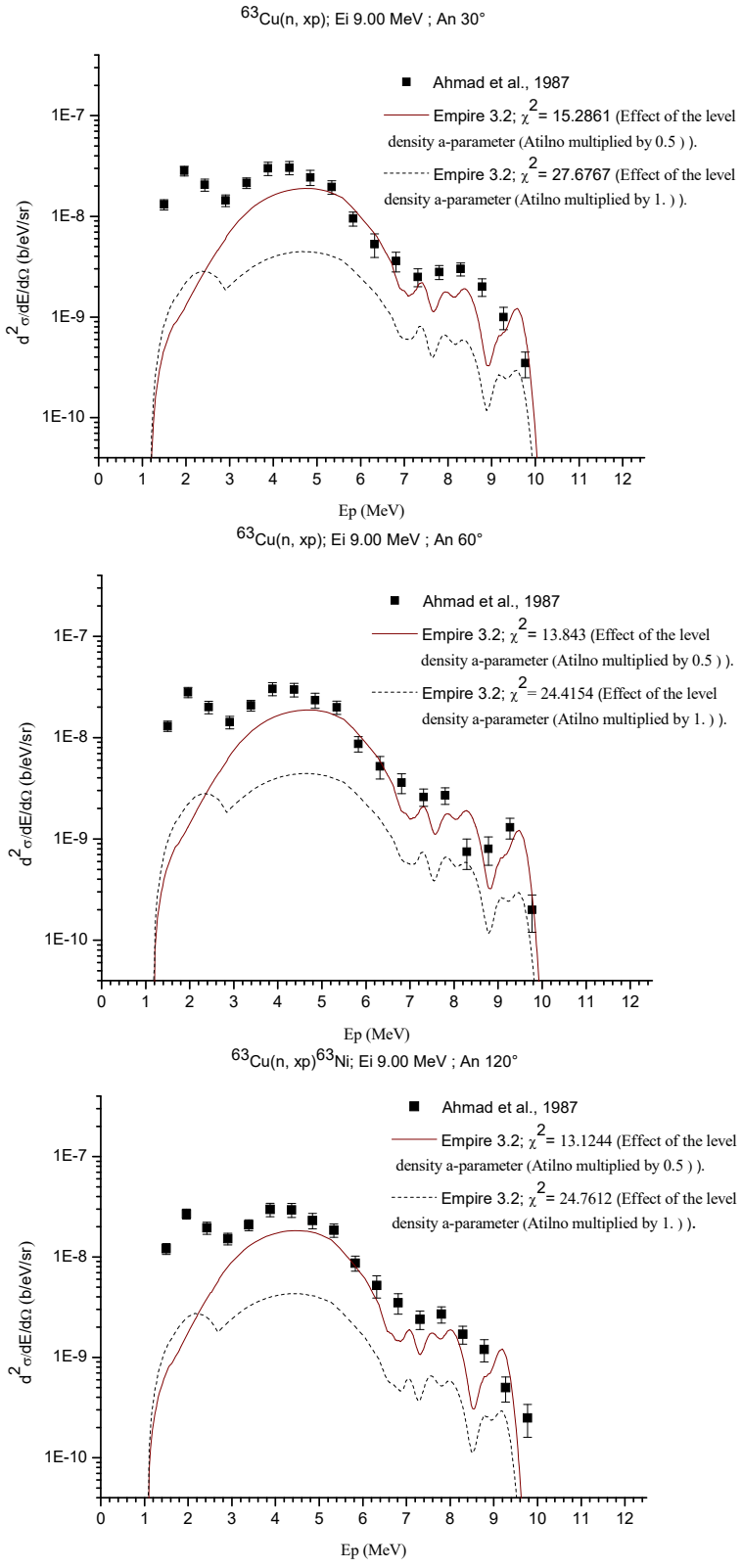

Fig. 1 Effect of the level density a-parameter on the proton emission spectrum for ^{63}Cu(n, xp) at 9 MeV incident neutron energy and at different emission angles (continuous and dashed lines) compared to the experimental data (solid squares) [13]

III. Results and Discussion

The calculated double differential cross sections for ^{63}Cu(n, xp) nuclear reaction at 9 and 11 MeV neutron incident energies and the proton emission spectra at 9 and 14.8 MeV have been illustrated in Figs. 1-6. We used the statistical model of the Hauser-Feshbach theory [9] to describe the equilibrium emission from the compound nucleus. In the framework of exciton model [5], we calculated the double differential cross sections and the proton emission with PCROSS module of the EMPIRE [1] combined with Kalbach angular distributions systematics [10].

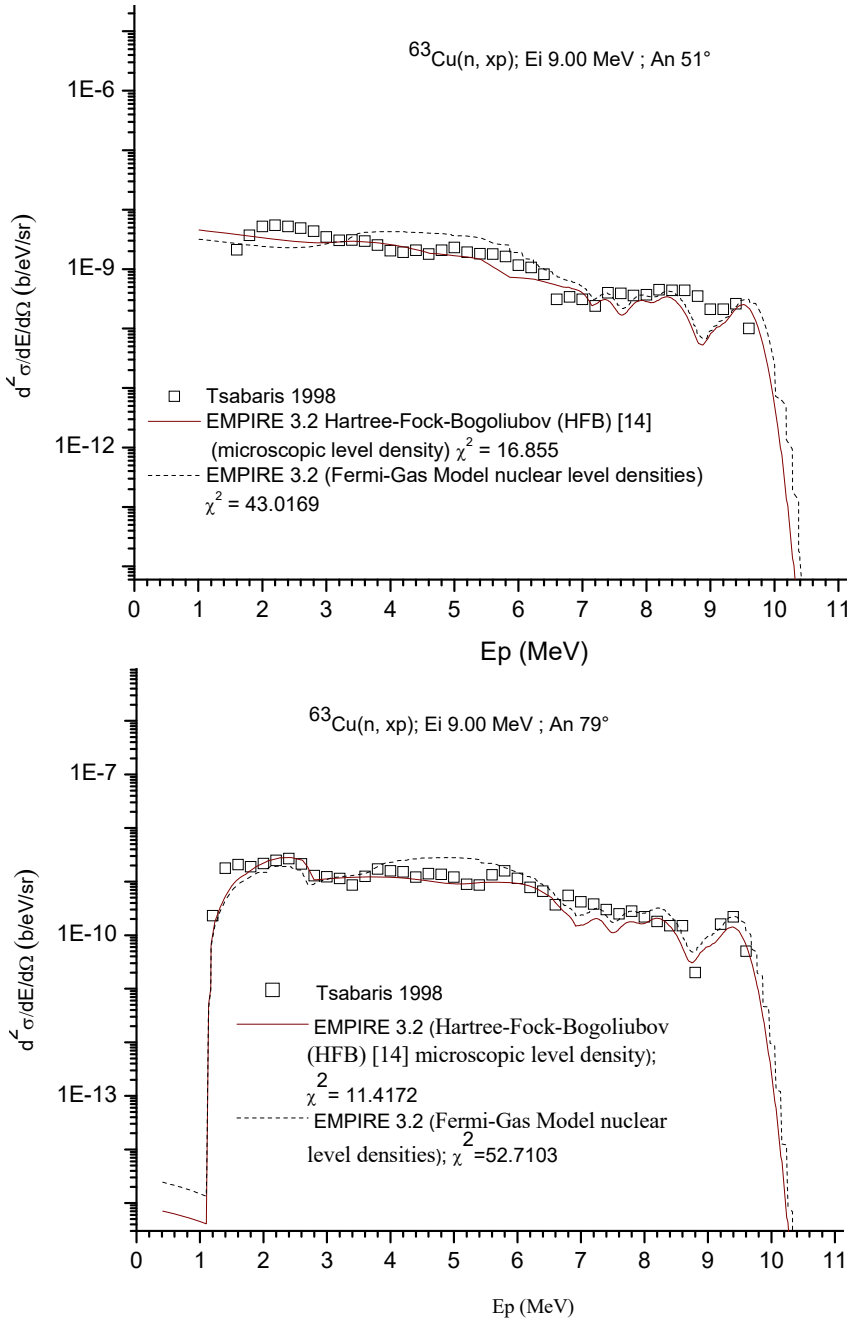

Fig. 2 (a) Comparison among double-differential cross sections as calculated with HFBM [14] (for 51- and 79-deg emission angles), and the Fermi Gas Model nuclear level densities

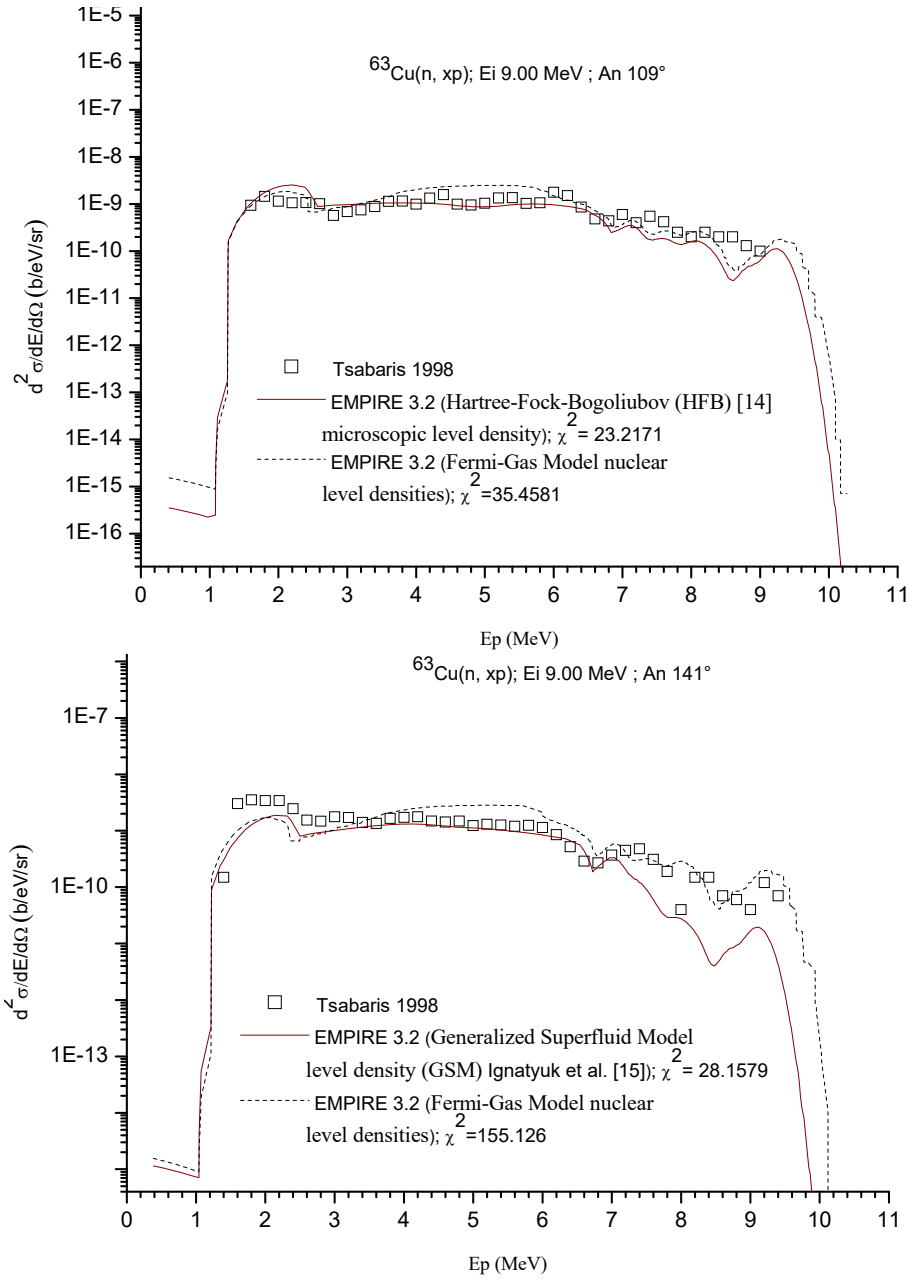

Fig. 2 (b) Comparison among double-differential cross sections as calculated with HFBM [14] (for 109-deg emission angle), the GSM level density [15] (for 141-deg emission angle), and the Fermi Gas Model nuclear level densities

At 9 MeV neutron incident energies for different angles emission (30°, 60° and 120°), the optical model parameters of [11] have been used for neutrons. For protons, the local and global nucleon optical models of [12] have been used. The Fermi-Gas Model nuclear level densities are very consistent in the cross sections calculated where the changes on the level density *a*-parameter affect the fit. This is done with the *Atilno* input parameter and the level density *a*-parameter has been multiplied by 0.50. The calculated cross sections were compared to the experimental data of [13] as shown in Fig. 1.

At the same 9 MeV neutron incident energies but at different angles emission (51°, 79°, 109° and 141°), the local and global nucleon optical models of [12] have been used for neutrons and protons. As shown in Figs. 2 (a) and (b), the microscopic level density of Hartree-Fock-Bogoliubov (HFB) [14] and the Generalized Superfluid Model (GSM) level density [15] affect the shape of the curves. The calculated double differential cross sections are in good agreement with the experimental data of [16].

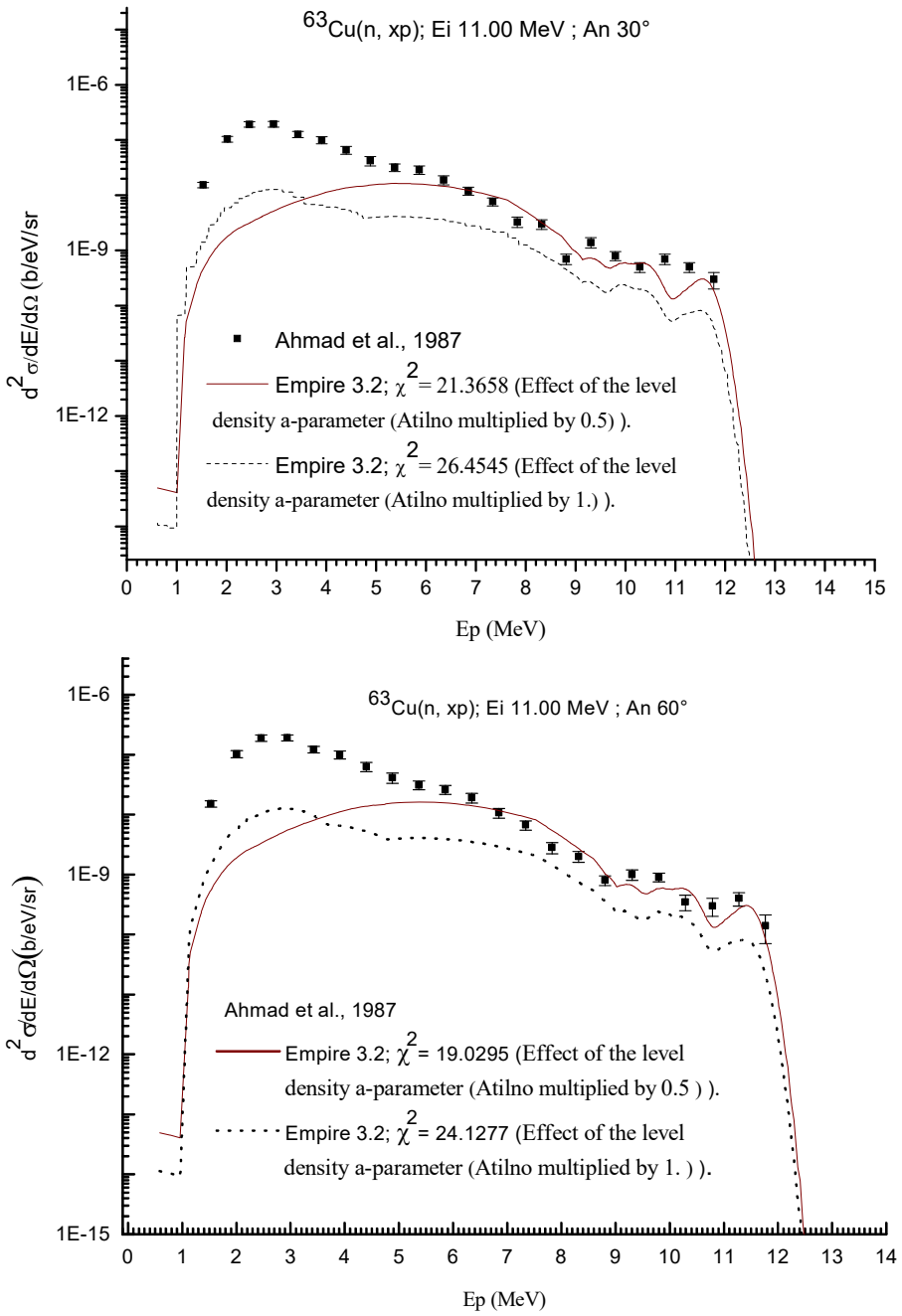

Fig. 3 (a) Effect of the level density a-parameter on the proton emission spectrum for ^{63}Cu(n, xp) reaction at 11-MeV incident neutron energy and at different emission angles (continuous and dashed lines) compared to the experimental data (solid squares) [13]

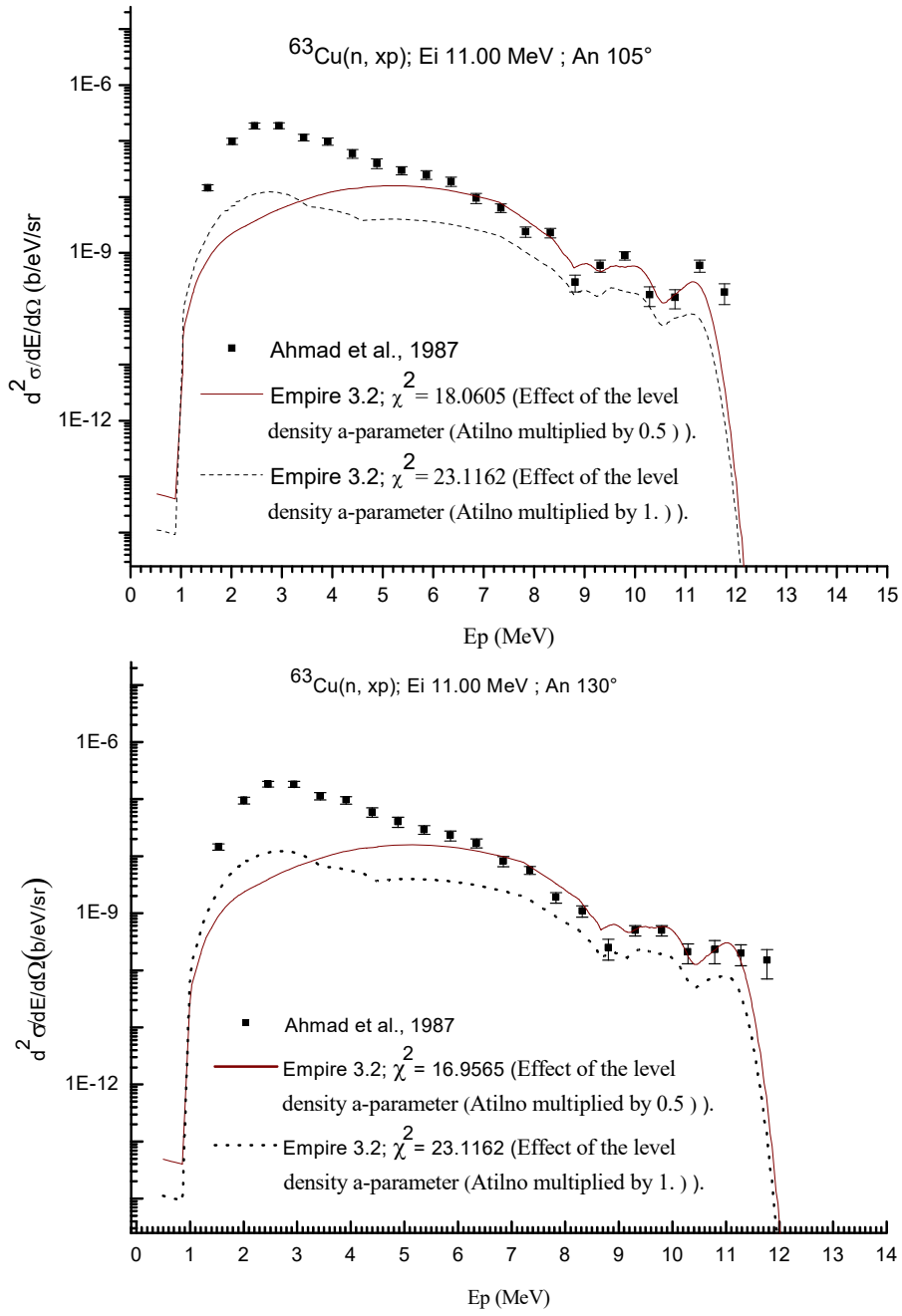

Fig. 3 (b) Effect of the level density a-parameter on the proton emission spectrum for ^{63}Cu(n, xp) reaction at 11-MeV incident neutron energy and at different emission angles (continuous and dashed lines) compared to the experimental data (solid squares) [13]

At 11 MeV neutron incident energies and for different angles emission (30°, 60°, 105° and 130°), the local and global nucleon optical models of [12] have been used for neutrons and protons. The double differential cross sections calculated are shown in Figs. 3 (a) and (b). However, the calculated results are inconsistent with the experimental data [13] below proton emission energy 4 and 6 MeV at 9 and 11 MeV neutron incident energies as shown in Figs. 1 and 3, respectively. We can say that at low energies, the equilibrium effect is small. The number of particle-hole pairs excited is small too and it increases with increasing incident energy. So the contribution of (n, xp) is more or less negligible below proton emission energy 4 and 6 MeV. The level density a-parameter modified is the best agreement with the experimental values [13] for the proton emission energy region above 4-11 MeV, and the contributions are from the (n, p) and (n, np) reactions cross sections.

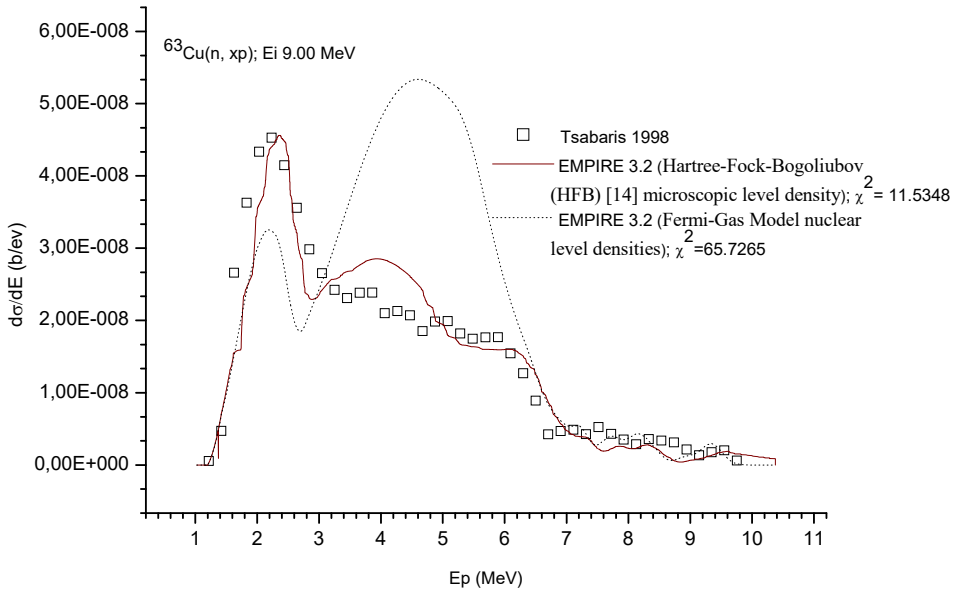

Fig. 4 Comparison between calculated angle-integrated proton particle emission spectra with HFBM [14] and Fermi Gas Model nuclear level density (continuous and dashed lines) for ^{63}Cu(n, xp) reaction to the experimental data (open squares) [16] from 9-MeV neutron energy induced using the Exciton Model [5]

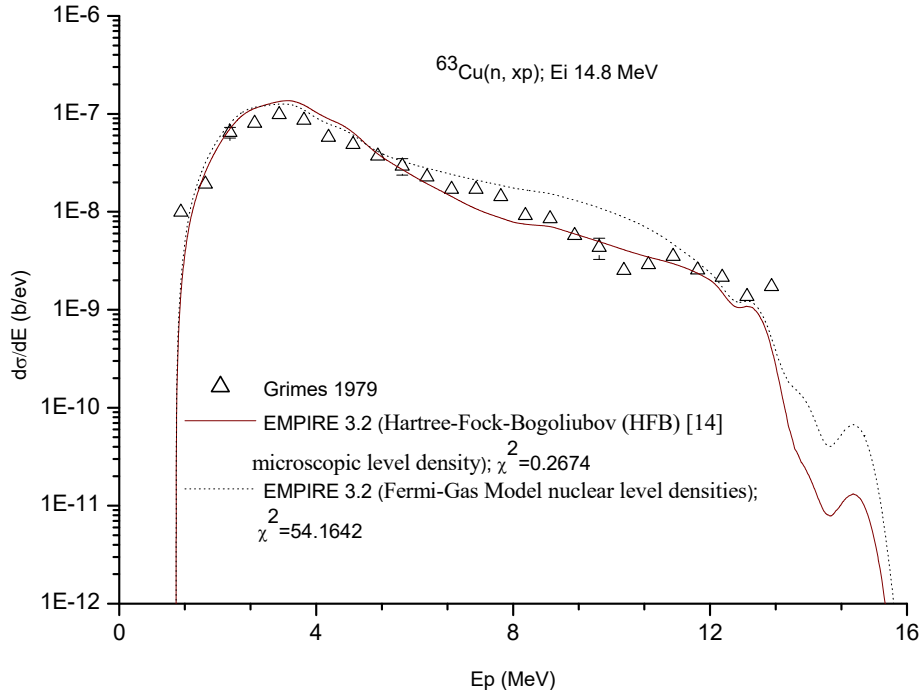

Fig. 5 Comparison between calculated angle-integrated proton particle emission spectra with HFBM [14] and Fermi Gas Model nuclear level density (continuous and dashed lines) for ^{63}Cu(n, xp) reaction to the experimental data [17] from 14.8-MeV neutron energy induced using the Exciton Model [5]

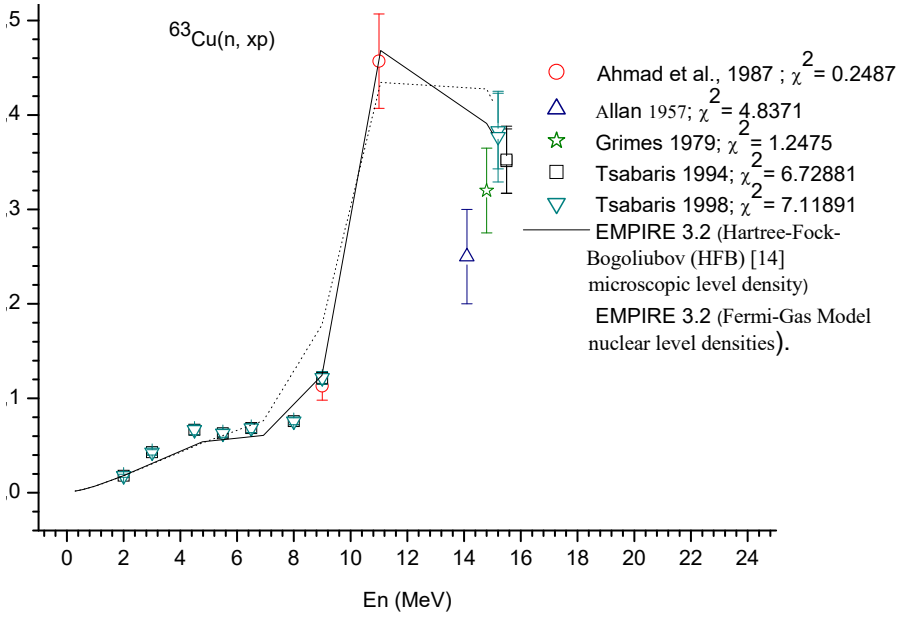

Fig. 6 Comparison between calculated total cross section with HFBM [14] and Fermi Gas Model nuclear level density (continuous and dashed lines) for ^{63}Cu(n, xp) reaction to the experimental data in neutron energy range from 2.0 to 15.5 MeV using the Exciton Model [5]

Fig. 4 shows the principal input parameters used in the Exciton Model (PCROSS) calculations. The local and global nucleon optical models of [12] have been used for neutrons and protons and the HFBM level density [14] is used. At incident neutron energies of 9 MeV, we obtain good agreement between our calculation and the experimental data of [16] as shown in Fig. 4.

Fig. 5 shows the proton emission energy spectra for n+ ^{63}Cu reaction at 14.8 MeV neutron energy, as measured by [17]. In our study, the Coupled Channels Method with the optical model parameters of [18] for direct inelastic scattering and the microscopic level density in terms of HFB model [14] have been used. The shape and magnitude of theoretical calculated results with EMPIRE 3.2 [1] are in good agreement with those of experimental data [16].

The calculated total cross section is in a good agreement compared to the experimental data [13], [16], [17], [19], [20] in neutron energy range from 2.0 to 15.5 MeV as shown in Fig. 6. Here, we used the same optical model and level density as used in proton emission energy spectra for n+ ^{63}Cu reaction at neutron energy 14.8 MeV.

For ^{65}Cu(n, xp) reaction, the phenomenological Gilbert-Cameron Model [21], the basic relations of the Fermi Gas Model, the GSM level density [15], the microscopic combinatorial level density HFB model of [14] and the Back Shifted Fermi Gas Model [22] as included in RIPL-3 [23], are used in this work. The calculated double-differential cross sections for the ^{65}Cu(*n*, *xp*) nuclear reaction at 9-and 11-MeV incident neutron energies, the proton emission spectra at 14.8 MeV and the calculated total cross section in neutron energy range from 9.0 to 15.0 MeV are illustrated in Figs. 7-10. We used a statistical model that is an advanced implementation of the Hauser-Feshbach theory [9] to describe the equilibrium emission from the compound nucleus. The local and global nucleon optical models of [12] have been used for neutrons and protons for all the calculations by using the TALYS code [2].

At 9-MeV incident neutron energy and for different emission angles (30°, 60° and 120°), the double-differential cross sections calculated are shown in Fig. 7. In the framework of exciton model [5] using PCROSS module of EMPIRE [1] combined with Kalbach angular distribution systematics [10], the optical model parameters of [11] have been used for neutrons and for protons, the optical model parameters of [24] have been chosen. The HFBM microscopic level density [14] is used. However, choosing the level density models and the number of discrete levels may fail; we may be forced to adjust the level density parameters themselves. These are done with the ROHFBA input parameter (HFB pseudo *a*-parameter to adjust numerical HFB level densities for nucleus), and set to -0.920 in ^{65}Cu. In the framework of HMS model [25] using DDHMS module of EMPIRE code [1], we choose the same microscopic level density HFBM [14], and we use the ROHFBP input parameter (HFB pairing-like parameter to shift in energy numerical HFB level densities for nucleus), that is set to –5.000 in all nuclei. The optical models for neutrons [11] and protons [24] are the same as those used in PCROSS module of EMPIRE code [1]. In the framework of TALYS code [2], the GSM level density [15] is used and the level density *a*-parameter is set to 5.1 in ^{65}Cu. The level density parameter for both level densities models (HFBM [14] and GSM [15]) affects the shape of the curves. At 9-MeV incident neutron energies, the results using the TALYS code [2] code for ^{65}Cu(*n*, *xp*) reaction are closer to experiment [13] than those used with the PCROSS and DDHMS modules of the EMPIRE code [1].

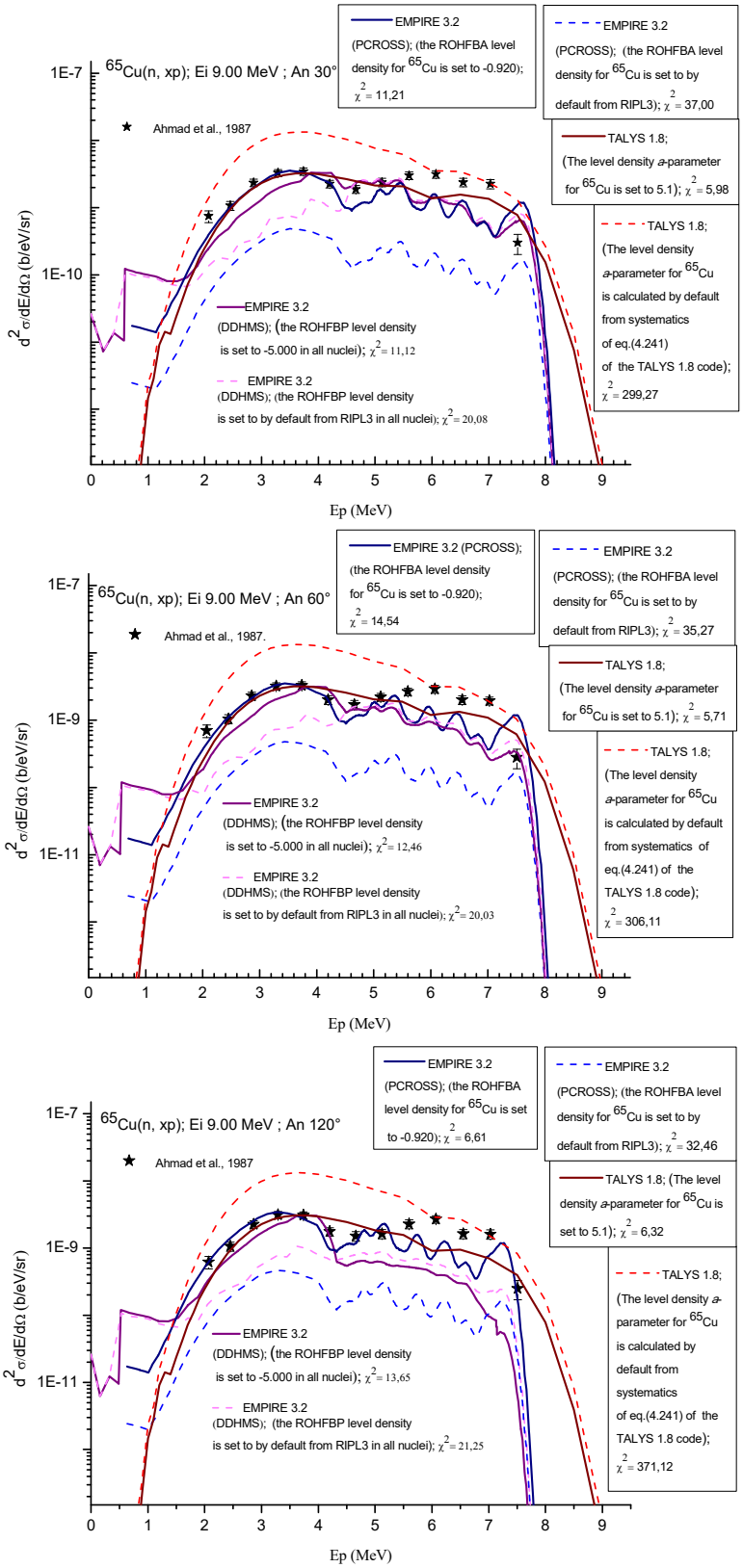

Fig. 7 Effect of the level density a-parameter on the proton emission spectrum for ^{65}Cu(*n*, *xp*) reaction at 9-MeV incident neutron energy and at different emission angles (continuous and dashed lines) compared to the experimental data [13] (solid stars)

At 11-MeV incident neutron energy and for different emission angles (30°, 60°, 105° and 130°), the optical models for neutrons and protons are the same as those used at 9-MeV incident neutron energies. The ROHFBA input parameter is set to -0.61 in ^{65}Cu in both PCROSS and DDHMS modules of EMPIRE code [1]. Using TALYS code [2], the level density *a*- parameter is set to 5.2 in ^{65}Cu. As shown in Figs. 8 (a) and (b), the level density parameter for the HFBM microscopic level density [14] and for the GSM level density [15] affects the shape of the curves.

As shown in Fig. 9, the optical model parameters of [26] have been used for neutrons and for protons, the optical model parameters of [27] have been chosen. The level density parameter for the Gilbert and Cameron Model [21] cannot be read as a single input entry. This is done with the Atilno input parameter, and the level density *a*-parameter has been multiplied by 1.04 by using the PCROSS module of EMPIRE code [1]. By using TALYS code [2], the level density *a*-parameter of the Fermi gas model modified has the best agreement with the experimental values [17] for the proton emission at 14.8-mev neutron energy.

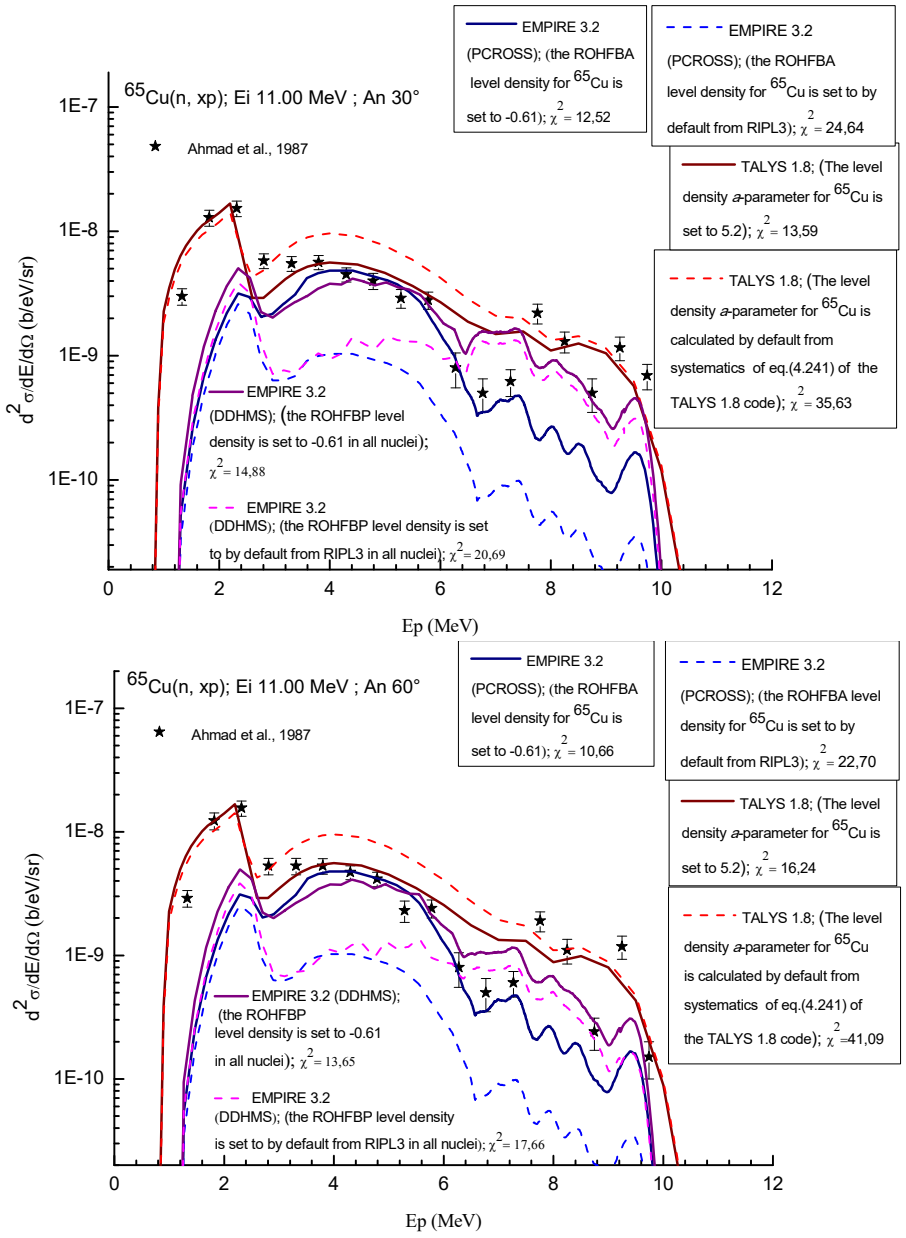

Fig. 8 (a) Effect of the level density a-parameter on the proton emission spectrum for ^{65}Cu(*n*, *xp*) reaction at 11-MeV incident neutron energy and at different emission angles (continuous and dashed lines) compared to the experimental data [13] (solid stars)

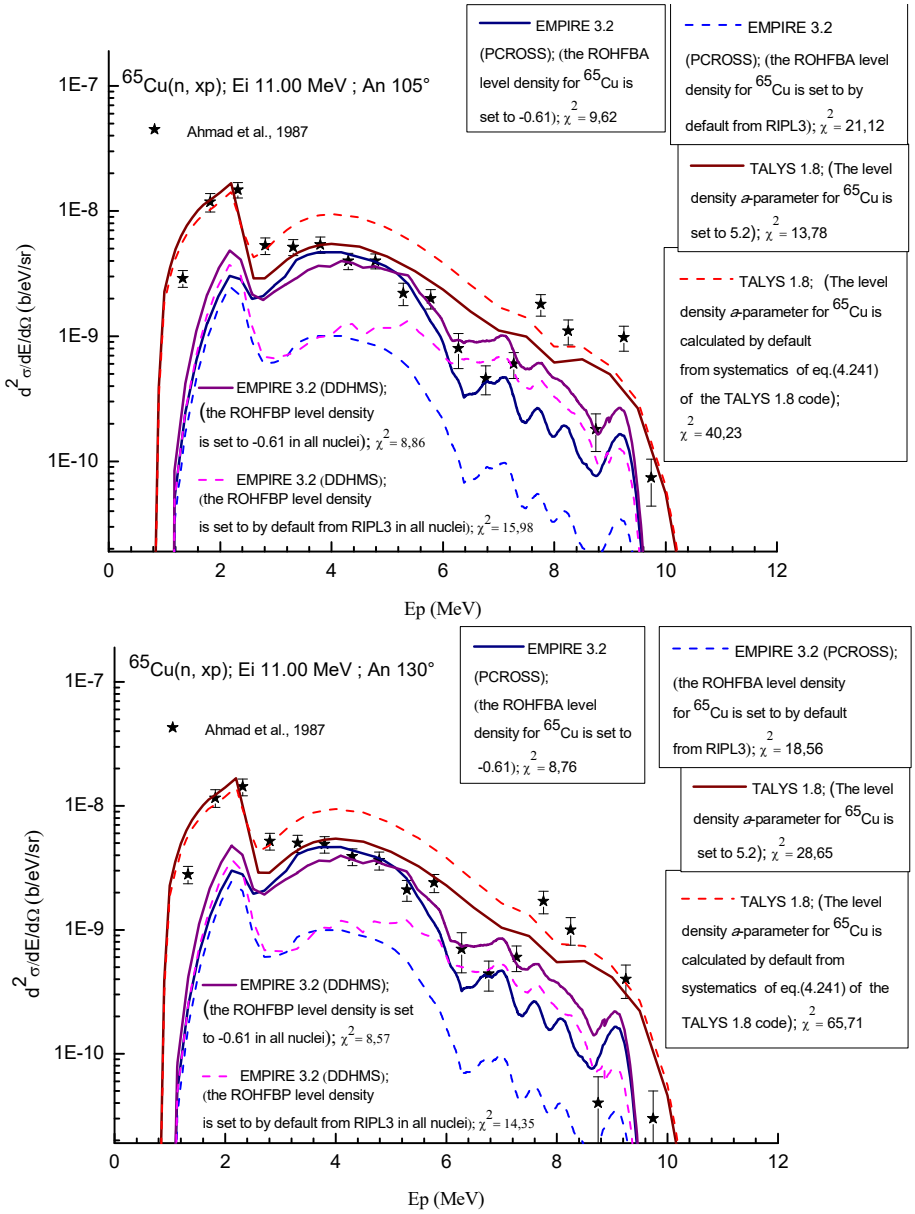

Fig.8 (b) Effect of the level density a-parameter on the proton emission spectrum for ^{65}Cu(*n*, *xp*) reaction at 11-MeV incident neutron energy and at different emission angles (continuous and dashed lines) compared to the experimental data [13] (solid stars)

The calculated total cross section in the neutron energy range from 2.0 to 15.5 MeV is shown in Fig. 10. By using the PCROSS module of EMPIRE code [1], the local and global nucleon optical models of [12] have been used for neutrons and protons. The level density of [21] used in PCROSS module of EMPIRE code [1] and the Back Shifted Fermi Gas Model [22] used in TALYS code [2] affect strongly the shape of the curve. The calculated total cross section is in a good agreement compared to the experimental data [13], [17], [20].

IV. Conclusion

For ^{63}Cu(n,xp) and ^{65}Cu(n,xp) reactions, we have analyzed the calculated double differential cross sections, angle-integrated calculations and the calculated proton emission cross section of (n, x) reactions on ^{63}Cu and ^{65}Cu targets using nuclear reaction model in EMPIRE 3.2 [1] and TALYS 1.8 codes [2]. Our results show that the calculations of the pre-equilibrium in terms of exciton model for ^{63}Cu(n, xp) and ^{65}Cu(n,xp) reactions show the similar behavior with the experimental data [13], [16], [17], [19], [20]. The calculated double differential cross sections for ^{65}Cu(n, xp)^{63}Ni reaction in terms of Hybrid Model Simulation (HMS) with the Ignatyuk systematics [25] are in a good agreement with the experimental result [13]. Also, the different level density models used and the changed on the level density *a*-parameter affect strongly the fit for ^{63}Cu(n, xp) and ^{65}Cu(n,xp) reactions.

For all the figures shown in this paper, the EMPIRE [1] and TALYS [2] results show that the lower χ^2 value gives a significantly better fit when compared to the experimental results [13], [16], [17], [19], [20].

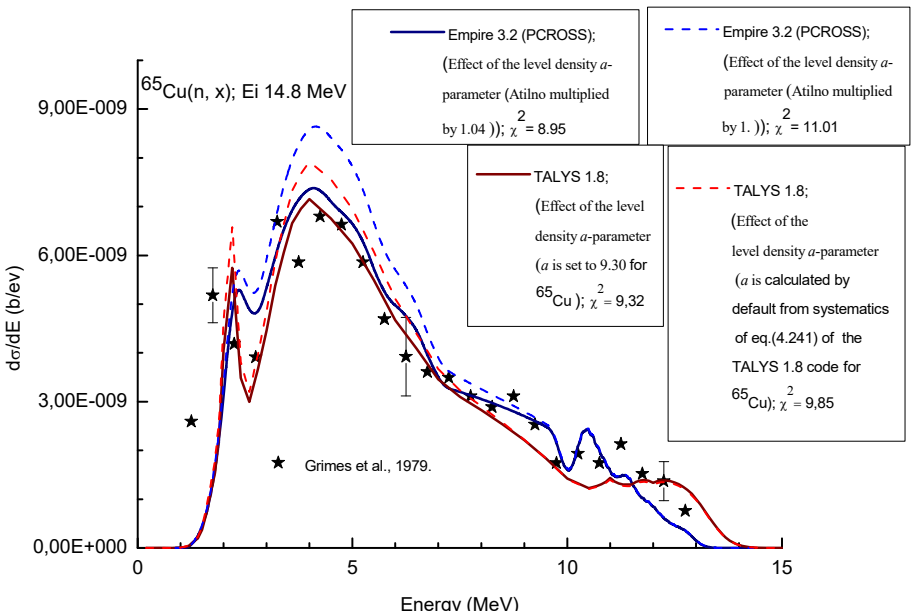

Fig. 9 Effect of the level density *a*-parameter on the proton emission spectrum for ^{65}Cu(*n*, *xp*) reaction at 14.8 MeV incident neutron energy (continuous and dashed lines) compared to the experimental data [17] (solid stars)

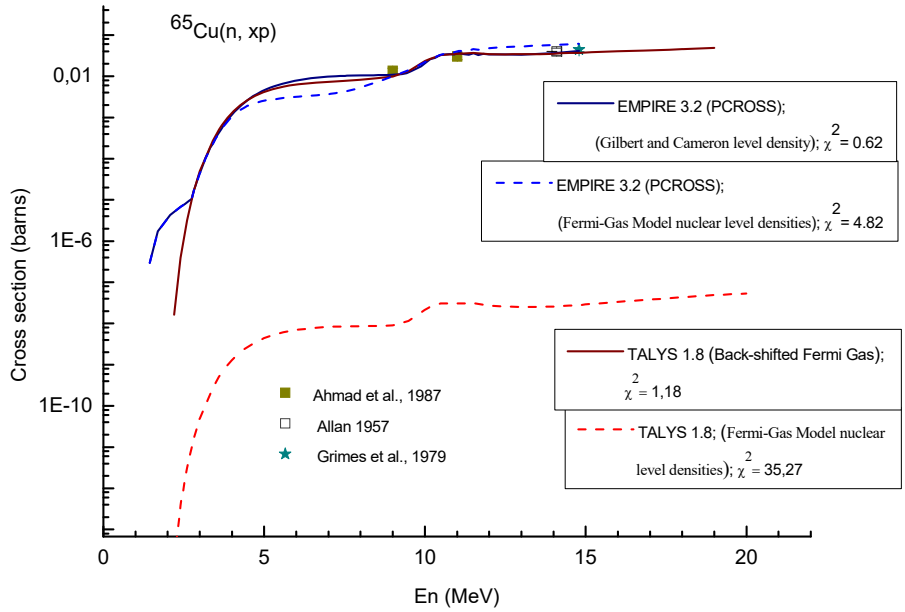

Fig. 10 Comparison between calculated total cross section with Gilbert and Cameron level density [21], Back-Shifted Fermi Gas [22] and Fermi Gas Model nuclear level density (continuous and dashed lines) for ^{65}Cu(*n*, *xp*) reaction to the experimental data [13], [17] and [20] in neutron energy range from 9.0 to 15.0 MeV using the Exciton Model [5]

References

[1] EMPIRE-3.2 (Malta) (August2013; *http://www.nndc.bnl.gov/empire/* (current as of July 12, 2015).

[2] J. Koning, S. Hilaire, and M. C. Duijvestijn, "Talys-1.0," *Proc. Int. Conf. Nuclear Data for Science and Technology (ND-2007)*, Nice, France, (April 22–27, 2007).

[3] L. Yettou, Preequilibrium models for ^{63}Cu(*n*, *xp*) Reaction in Neutrons at 9, 11, 14.8 and 15 MeV Using the EMPIRE 3.2 Code, Nucl. Sci. Eng, 183. 275-285. (June 2016).

[4] L. Yettou, Calculation of pre-equilibrium effects in neutron-induced cross section on ^{65}Cu, ND 2016: *International Conference on Nuclear Data for Science and Technology*, Bruges, Belgium ; *EPJ Web of Conferences*, Volume 146, id. 12024.

[5] J. J. Griffin, *Phys. Rev. Lett*., 17, 478 (1966); *http//dx.doi.org/10.1103/PhysRevLett*.17.478.
[6] C. K. Cline and M. Blann *Nucl. Phys. A*, 172, 225 (1971); *http://dx.doi.org*/10.1016/0375-9474(71)90713-5.
[7] C. K. Cline *Nucl. Phys. A*, 193, 417 (1972); *http://dx.doi.org*/10.1016/0375-9474(72)90330-2.
[8] I. RIBANSKY, P. OBLOZINSKY, and E. BETAK, *Nucl. Phys. A*, 205, 545 (1973); *http://dx.doi.org*/10.1016/0375-9474(73)90705-7.
[9] W. Hauser and H. Feshbach, *Phys. Rev*., 87, 366(1952),*http://dx.doi.org*/10.1103/PhysRev.87.366; see also L. WOLFENSTEIN, *Phys. Rev*., 82, 690 (1951), *http://dx.doi.org*/10.1103/*PhysRev*.82.690.
[10] C. Kalbach, "Systematics of Continuum Angular Distributions: Extensions to Higher Energies," *Phys. Rev. C*, 37, 2350(1988); *http://dx.doi.org*/10.1103/*PhysRevC*.37.2350.
[11] J. P. Delaroche et al., *Nucl. Phys. A*, 390, 541 (1982); *http://dx.doi.org*/10.1016/0375-9474(82)90282-2.
[12] A. J. Koning and J. P. Delaroche, "Local and Global Nucleon Optical Models from 1 keV to 200 MeV,"*Nucl. Phys. A*, 713, 231 (2003); *http://dx.doi.org*/10.1016/S0375-9474(02)01321-0.
[13] M. Ahmad et al., "Charged-Particle Emission in Reactions of 9- and 11-MeV Neutrons with ^{63,65}Cu,"*Nucl. Sci.Eng*., 95, 296 (1987); *http://dx.doi.org*/10.13182/*NSE*95-296.
[14] S. Goriely, M. Samyn, and J. M. Pearson,*Phys. Rev. C*, 75, 064312 (2007); *http://dx.doi.org*/10.1103/PhysRevC.75.064312.
[15] A. V. Ignatyuk, G. N. Smirenkin, and A. S.Tishin, *Sov. J. Nucl. Phys*., 21, 255 (1975).
[16] C. Tsabaris et al., "Measured and Calculated Differential and Total Yield Cross-Section Data of ^{58}Ni(n,x) and ^{63}Cu(n,xp) in the Neutron Energy Range from 2.0 to 15.6 MeV,"*Nucl. Sci. Eng*., 128, 1, 47 (1998); *http://dx.doi.org*/10.13182/*NSE*128-47.
[17] S. M. Grimes et al., "Charged-Particle Emission in Reactions of 15-MeV Neutrons with Isotopes of Chromium, Iron, Nickel, and Copper,"*Phys. Rev. C*, 19, 2127 (1979); *http://dx.doi.org*/10.1103/PhysRevC.19.2127.
[18] B. Morillon and P. Romain, "Bound Single-Particle States and Scattering of Nucleons on Spherical Nuclei with a Global Optical Model,"*Phys. Rev. C*, 76, 044601 (2007); *http://dx.doi.org*/10.1103/*PhysRevC*.76.044601.
[19] C. Tsabaris, E. Wattecamps, and G. Rollin, "Double Differential (n,xp) and (n,x alpha) Cross Section Measurements of Al-27, Ni-58 and Cu-63 in the Neutron Energy Range from 2.0 to 15.5 MeV,"*Proc. Conf. Nuclear Data for Science and Technology*, Gatlinburg, Tennessee, May 9 –13, 1994, p. 282, *American Nuclear Society* (1994).
[20] D. L. Allan, "Protons from the Interaction of 14 MeV Neutrons with Medium Weight Nuclei,"*Proc. Phys. Soc. A*, 70, 195 (1957); *http://dx.doi.org*/10.1088/0370-1298/70/3/305.
[21] A. Gilbert and A. G. W. Cameron,Can. J. Phys., 43, 1446 (1965);http://dx.doi.org/10.1139/p65-139.
[22] W. Dilg, W. Schantl, H. Vonach, and M. Uhl, *Nucl. Phys. A*217, 269 (1973).
[23] R. Capote et al., "Reference Input Parameter Library (RIPL-3),"*Nucl. Data Sheets*, 110, 12, 3107 (2009); *http://dx.doi.org*/10.1016/j.nds.2009.10.004.
[24] Xiaohua Li and Chonghai Cai, *Nucl. Phys. A* 801, 43-67 (2008)
[25] M. Blann, *Phys. Rev. C*, 54, 1341 (1996); *http://dx.doi.org*/10.1103/*PhysRevC*.54.1341.
[26] R. L. Varner, W.J. Thompson, T.L. McAbee, E.J. Ludwig, T.B. Clegg, *Phys. Rep*. 201, 57 (1991)
[27] S. Kailas et al., *Phys. Rev. C* 20, 1272(1979); *Pramana. J.Phys*. 27, 139(1986)